Analysis of Sharp Metal Edge Diagonal to the Cell Cube in FDTD Grid

Feng Lu, Bin Chen, Yun Yi, Cheng Gao, Li-Hua Shi, and Bi-Hua Zhou

***Abstract*—The finite-difference time-domain(FDTD) update equations for sharp metal edges [1] are extended in this paper. New FDTD update equations for sharp metal edges diagonal to cell cube in FDTD grid are presented. Unlike the literature [1], the edge is assumed to be not parallel to any cell face. A dramatic improvement in computed accuracy was observed when a stripline with two sharp edges diagonal to the cell cube in FDTD grid was analyzed using the new equations.**

***Index Terms*—Edge, FDTD, microstrip, singular, strip.**

I. Introduction

THE finite-difference time-domain (FDTD) method has been applied to many electromagnetic problems in antennas, scattering and microwave circuit components. In dealing with flat metal surface, where the sharp metal edges of metal surface do not coincide with finite difference grid lines, the staircase approximation is commonly used. But this technique is not accurate if the grid is too coarse. To overcome the difficulties in the staircase approximation, many techniques have been proposed and applied to various problems [2]–[5]. In 1999, Esselle [1] presented the new FDTD update equations for sharp metal edges. In his technique, the edge is assumed to be diagonal to the Yee cell faces. The new singularity-enhanced FDTD equations generate highly accurate results with no noticeable extra cost in computing time and memory. In this paper we extend this technique to sharp metal edges diagonal to cell cubes in FDTD grid. The edge is assumed to be not parallel to any cell face but coincide with the diagonal of cell cube.

The same example as [1] was used to test the accuracy of the new equations, with the structure assumed to be at an angle of 45° to a coordinate plane (xoy). The stability of the new equations was tested by analyzing microstrip in homogeneous and inhomogeneous media.

II. Theory

The finite-difference element near metal sheet is shown in Fig. 1, where the FDTD grid is parallel to x, y and z axes. The metal sheet is at an angle α_1 (where $\alpha_1 = 45°$) to the xoy plane, with its edge running diagonally across the cube of FDTD cells. In order to describe the quasi-static electromagnetic field near the sharp metal edge in the coordinate x, y, z, a new coordinate system (coordinate x', y', z') is set up. In the new coordinate system, z'-axis coincide with metal edge, x'-axis placed in metal sheet is perpendicular to z'-axis. y'-axis is perpendicular to $x'o'z'$ plane. We can set up the relation between two coordinate systems through a 3×3 matrix

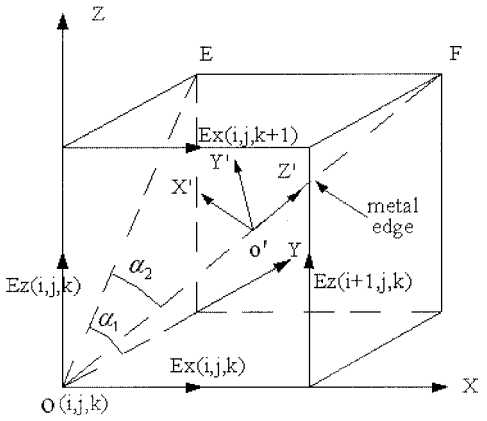

Fig. 1. Finite-difference element near metal edge.

$$\begin{bmatrix} x \\ y \\ z \end{bmatrix} = \begin{bmatrix} -\cos\alpha_2 & 0 & \sin\alpha_2 \\ \cos\alpha_1 \sin\alpha_2 & -\sin\alpha_1 & \cos\alpha_1 \cos\alpha_2 \\ \sin\alpha_1 \sin\alpha_2 & \cos\alpha_1 & \sin\alpha_1 \cos\alpha_2 \end{bmatrix} \begin{bmatrix} x' \\ y' \\ z' \end{bmatrix} \tag{1}$$

where α_1 is the angle measured from y-axis to line OE, α_2 is the angle measured from metal edge to line OE. According to Van Bladel's expressions [1], [6] and the (1), we can get the quasi-static electromagnetic field near the sharp metal edge in the coordinate x, y, z as follows:

$$E_x = -\frac{B}{\sqrt{r}}\left(\cos\alpha_2 \cdot \sin\frac{\alpha}{2}\right) \tag{2a}$$

$$E_y = \frac{B}{\sqrt{r}}\left(\cos\alpha_1 \cdot \sin\alpha_2 \cdot \sin\frac{\alpha}{2} + \sin\alpha_1 \cdot \cos\frac{\alpha}{2}\right) \tag{2b}$$

$$E_z = \frac{B}{\sqrt{r}}\left(\sin\alpha_1 \cdot \sin\alpha_2 \cdot \sin\frac{\alpha}{2} - \cos\alpha_1 \cdot \cos\frac{\alpha}{2}\right) \tag{2c}$$

$$H_x = \frac{A}{\sqrt{r}}\left(\cos\alpha_2 \cdot \cos\frac{\alpha}{2}\right) \tag{2d}$$

$$H_y = \frac{-A}{\sqrt{r}}\left(\cos\alpha_1 \cdot \sin\alpha_2 \cdot \cos\frac{\alpha}{2} - \sin\alpha_1 \cdot \sin\frac{\alpha}{2}\right) \tag{2e}$$

$$H_z = \frac{-A}{\sqrt{r}}\left(\sin\alpha_1 \cdot \sin\alpha_2 \cdot \cos\frac{\alpha}{2} + \cos\alpha_1 \cdot \sin\frac{\alpha}{2}\right) \tag{2f}$$

where A, B are unknown constant, r is the distance from the edge to the field point, α is the angle measured from the metal sheet [1].

Manuscript received September 27, 2002; revised December 27, 2002. This work was supported by National Science Foundation of China under Grant 69971024. The review of this letter was arranged by Associate Editor Dr. Rüdiger Vahldieck.

The authors are with the Electromagnetic Laboratory, Nanjing Engineering Institute, Nanjing 210007, China.

Digital Object Identifier 10.1109/LMWC.2003.815286

According to the K. P. Esselle's method [1], we can get new FDTD update equations as follows:

$$h^{n+1/2}_{x1|i,j,k} = h^{n-1/2}_{x1|i,j,k} - 2\cdot\frac{\Delta t}{\mu\cdot\Delta}\cdot\left(c3\cdot e^{n}_{z|i,j+1,k} + c4\cdot e^{n}_{y|i,j,k}\right)$$

$$h^{n+1/2}_{x2|i,j,k} = h^{n-1/2}_{x2|i,j,k} + 2\cdot\frac{\Delta t}{\mu\cdot\Delta}\cdot\left(c3\cdot e^{n}_{y|i,j,k+1} + c4\cdot e^{n}_{z|i,j,k}\right)$$

$$h^{n+1/2}_{x|i,j-1,k-1} = 0$$

$$h^{n+1/2}_{x|i,j,k-1} = h^{n-1/2}_{x|i,j,k-1} - \frac{\Delta t}{\mu\cdot\Delta}\cdot\left[c1\cdot\left(e^{n}_{y|i,j,k-1} + e^{n}_{z|i,j+1,k-1}\right) - c2\cdot\left(e^{n}_{y|i,j,k} + e^{n}_{z|i,j,k-1}\right)\right]$$

$$h^{n+1/2}_{x|i,j-1,k} = h^{n-1/2}_{x|i,j-1,k} + \frac{\Delta t}{\mu\cdot\Delta}\cdot\left[c1\cdot\left(e^{n}_{y|i,j-1,k+1} + e^{n}_{z|i,j-1,k}\right) - c2\cdot\left(e^{n}_{y|i,j-1,k} + e^{n}_{z|i,j,k}\right)\right]$$

$$h^{n+1/2}_{y|i,j,k} = h^{n-1/2}_{y|i,j,k} + \frac{\Delta t}{\mu\cdot\Delta}\cdot\left[c3\cdot\left(e^{n}_{z|i+1,j,k} - e^{n}_{x|i,j,k+1}\right) + c4\cdot\left(e^{n}_{x|i,j,k} - e^{n}_{z|i,j,k}\right)\right]$$

$$h^{n+1/2}_{y|i-1,j,k-1} = h^{n-1/2}_{y|i-1,j,k-1} + \frac{\Delta t}{\mu\cdot\Delta}\cdot\left[c3\cdot\left(e^{n}_{x|i-1,j,k-1} - e^{n}_{z|i-1,j,k-1}\right) + c4\cdot e^{n}_{z|i,j,k-1}\right]$$

$$h^{n+1/2}_{y|i,j,k-1} = h^{n-1/2}_{y|i,j,k-1} + \frac{\Delta t}{\mu\cdot\Delta}\cdot\left[c1\cdot\left(e^{n}_{x|i,j,k-1} + e^{n}_{z|i+1,j,k-1}\right) - c2\cdot\left(e^{n}_{z|i,j,k-1} + e^{n}_{x|i,j,k}\right)\right]$$

$$h^{n+1/2}_{y|i-1,j,k} = h^{n-1/2}_{y|i-1,j,k} - \frac{\Delta t}{\mu\cdot\Delta}\cdot\left[c1\cdot\left(e^{n}_{x|i-1,j,k+1} + e^{n}_{z|i-1,j,k}\right) - c2\cdot e^{n}_{z|i,j,k}\right]$$

$$h^{n+1/2}_{z|i,j,k} = h^{n-1/2}_{z|i,j,k} - \frac{\Delta t}{\mu\cdot\Delta}\cdot\left[c3\cdot\left(e^{n}_{y|i+1,j,k} - e^{n}_{x|i,j+1,k}\right) + c4\cdot\left(e^{n}_{x|i,j,k} - e^{n}_{y|i,j,k}\right)\right]$$

$$h^{n+1/2}_{z|i-1,j-1,k} = h^{n-1/2}_{z|i-1,j-1,k} - \frac{\Delta t}{\mu\cdot\Delta}\cdot\left[c3\cdot\left(e^{n}_{x|i-1,j-1,k} - e^{n}_{y|i-1,j-1,k}\right) + c4\cdot e^{n}_{y|i,j-1,k}\right]$$

$$h^{n+1/2}_{z|i-1,j,k} = h^{n-1/2}_{z|i-1,j,k} + \frac{\Delta t}{\mu\cdot\Delta}\cdot\left[c1\cdot\left(e^{n}_{x|i-1,j+1,k} + e^{n}_{y|i-1,j,k}\right) - c2\cdot e^{n}_{y|i,j,k}\right]$$

$$h^{n+1/2}_{z|i,j-1,k} = h^{n-1/2}_{z|i,j-1,k} - \frac{\Delta t}{\mu\cdot\Delta}\cdot\left[c1\cdot\left(e^{n}_{x|i,j-1,k} + e^{n}_{y|i+1,j-1,k}\right) - c2\cdot\left(e^{n}_{y|i,j-1,k} + e^{n}_{x|i,j,k}\right)\right]$$

$$e^{n+1}_{x|i,j+1,k+1} = 0$$

$$e^{n+1}_{x|i,j,k} = e^{n}_{x|i,j,k} - \frac{\Delta t}{\varepsilon\cdot\Delta}\cdot\left[c3\cdot\left(h^{n+1/2}_{z|i,j-1,k} - h^{n+1/2}_{y|i,j,k-1}\right) + c4\cdot\left(h^{n+1/2}_{y|i,j,k} - h^{n+1/2}_{z|i,j,k}\right)\right]$$

$$e^{n+1}_{x|i,j,k+1} = e^{n}_{x|i,j,k+1} - \frac{\Delta t}{\varepsilon\cdot\Delta}\cdot\left[c1\cdot\left(h^{n+1/2}_{z|i,j-1,k+1} + h^{n+1/2}_{y|i,j,k+1}\right) - c2\cdot\left(h^{n+1/2}_{y|i,j,k} + h^{n+1/2}_{z|i,j,k+1}\right)\right]$$

$$e^{n+1}_{x|i,j+1,k} = e^{n}_{x|i,j+1,k} + \frac{\Delta t}{\varepsilon\cdot\Delta}\cdot\left[c1\cdot\left(h^{n+1/2}_{z|i,j+1,k} + h^{n+1/2}_{y|i,j+1,k-1}\right) - c2\cdot\left(h^{n+1/2}_{y|i,j+1,k} + h^{n+1/2}_{z|i,j,k}\right)\right]$$

$$e^{n+1}_{y|i,j,k} = e^{n}_{y|i,j,k} + \frac{\Delta t}{\varepsilon\cdot\Delta}\cdot\left[c3\cdot\left(h^{n+1/2}_{z|i-1,j,k} - h^{n+1/2}_{x|i,j,k-1}\right) + c4\cdot\left(h^{n+1/2}_{x1|i,j,k} - h^{n+1/2}_{z|i,j,k}\right)\right]$$

$$e^{n+1}_{y|i+1,j,k+1} = e^{n}_{y|i+1,j,k+1} + \frac{\Delta t}{\varepsilon\cdot\Delta}\cdot\left[c3\cdot\left(h^{n+1/2}_{x|i+1,j,k+1} - h^{n+1/2}_{z|i+1,j,k+1}\right) + c4\cdot h^{n+1/2}_{z|i,j,k+1}\right]$$

$$e^{n+1}_{y|i+1,j,k} = e^{n}_{y|i+1,j,k} - \frac{\Delta t}{\varepsilon\cdot\Delta}\cdot\left[c1\cdot\left(h^{n+1/2}_{x|i+1,j,k-1} + h^{n+1/2}_{z|i+1,j,k}\right) - c2\cdot\left(h^{n+1/2}_{z|i,j,k}\right)\right]$$

$$e^{n+1}_{y|i,j,k+1} = e^{n}_{y|i,j,k+1} + \frac{\Delta t}{\varepsilon\cdot\Delta}\cdot\left[c1\cdot\left(h^{n+1/2}_{x|i,j,k+1} + h^{n+1/2}_{z|i-1,j,k+1}\right) - c2\cdot\left(h^{n+1/2}_{z|i,j,k+1} + h^{n+1/2}_{x2|i,j,k}\right)\right]$$

$$e^{n+1}_{z|i,j,k} = e^{n}_{z|i,j,k} + \frac{\Delta t}{\varepsilon\cdot\Delta}\cdot\left[c3\cdot\left(h^{n+1/2}_{x|i,j-1,k} - h^{n+1/2}_{y|i-1,j,k}\right) + c4\cdot\left(h^{n+1/2}_{y|i,j,k} - h^{n+1/2}_{x2|i,j,k}\right)\right]$$

$$
\begin{aligned}
e^{n+1}_{z|i+1,j+1,k} =& e^{n}_{z|i+1,j+1,k} + \frac{\Delta t}{\varepsilon \cdot \Delta} \\
&\cdot \left[c3 \cdot \left(h^{n+1/2}_{y|i+1,j+1,k} - h^{n+1/2}_{x|i+1,j+1,k} \right) \right. \\
&\left. - c4 \cdot h^{n+1/2}_{y|i,j+1,k} \right] \\
e^{n+1}_{z|i+1,j,k} =& e^{n}_{z|i+1,j,k} + \frac{\Delta t}{\varepsilon \cdot \Delta} \\
&\cdot \left[c1 \cdot \left(h^{n+1/2}_{x|i+1,j-1,k} + h^{n+1/2}_{y|i+1,j,k} \right) \right. \\
&\left. - c2 \cdot h^{n+1/2}_{y|i,j,k} \right] \\
e^{n+1}_{z|i,j+1,k} =& e^{n}_{z|i,j+1,k} - \frac{\Delta t}{\varepsilon \cdot \Delta} \\
&\cdot \left[c1 \cdot \left(h^{n+1/2}_{y|i-1,j+1,k} + h^{n+1/2}_{x|i,j+1,k} \right) \right. \\
&\left. - c2 \cdot \left(h^{n+1/2}_{y|i,j+1,k} + h^{n+1/2}_{x1|i,j,k} \right) \right]
\end{aligned}
$$

where $c1 = 0.931\,39$, $c2 = 1.313\,20$, $c3 = 1.060\,66$, $c4 = 1.495\,46$. Due to the symmetry of the fields near the metal edges, only four coefficients are involved in the new update equations. Equations of other FDTD nodes(l, m, n) situated in metal sheet are obtained by replacing l with i, replacing m with j and replacing n with k in all equations.

III. Numerical Results and Discussion

The accuracy of the new equations was tested by simulating wave propagation in a homogeneous strip line shown in Fig. 2. The width of the strip used is $0.8 \cdot \sin(\beta) = 0.8 \cdot \sqrt{2}/\sqrt{3} = 0.653\,\text{mm}$. It is embedded in a $\varepsilon_r = 4$ medium, which is sandwiched between two infinite ground planes. The gap between the strip and the lower and upper ground planes are 0.4 and 0.6 mm, respectively. The structure is at angle α_1 $(\alpha_1 = 45°)$ to the xoy plane, and its edge runs diagonally across the cube of FDTD cells. A relatively coarse cubic grid with $= 0.2\,\text{mm}$ was used in all cases.

The propagation constant $\beta(\omega)$ and the effective dielectric constant [4], [7] $\varepsilon_{eff}(\omega) = \beta^2(\omega)/\omega^2\mu_0\varepsilon_0$ of the TEM mode of the strip line were calculated using: 1) standard FDTD equations with staircase approximation near the two edges of strip; 2) new FDTD equations near the two edges of strip. In both 1) and 2), the conformal or split-cell FDTD equations [8] were used for the split cell near the metal sheet, and standard equations were used for all other nodes. The calculated effective dielectric constant is plotted in Fig. 3 against frequency. Note that the exact value of ε_{eff} is 4.0 at all frequency. It can be seen that the new FDTD equations have dramatically improved the accuracy of calculated ε_{eff}. The error in the 15–60 GHz range is 0.25%, which is much lower compared with 20% using 1).

In order to test the stability of the new equations, a variety of homogeneous stripline and inhomogeneous microstrip lines have been analyzed. This technique was also used in a radiator with sharp long metal edge. In all the tests, no instability was observed when we extended the time steps.

IV. Conclusion

In this paper, we extend Esselle's technique to sharp metal edges diagonal to the cell cube in FDTD grid. Compared with the standard FDTD technique, the new singularity-enhanced FDTD equations improve the computed accuracy dramatically without extra cost in computing time and memory. Due to the symmetry of the fields near the metal edges, the new equations only involve four coefficients. Therefore they can be easily implemented in standard FDTD software, and can be used to model any plane metal structure with sharp diagonal metal edges in cubic FDTD grid.

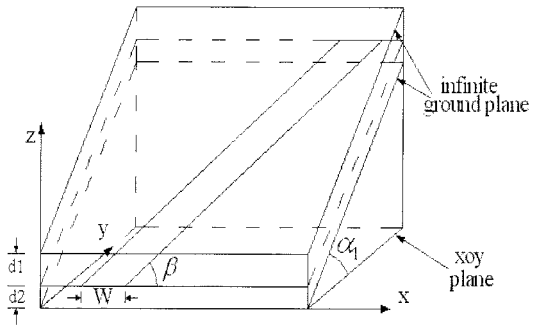

Fig. 2. Structure of the stripline ($\alpha_1 = 45°$, $\beta = \cos^{-1}(1/\sqrt{3})$).

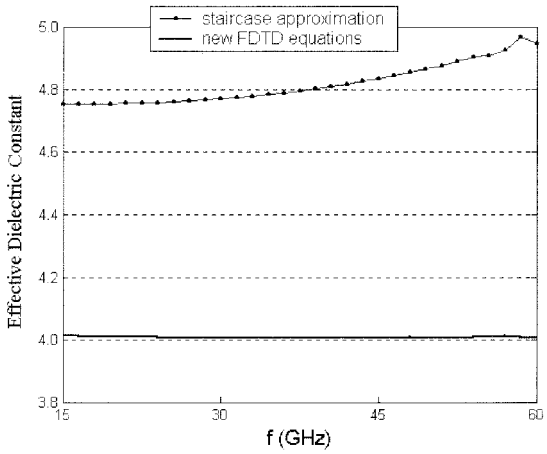

Fig. 3. Calculated effective dielectric constant of the stripline.

References

[1] K. P. Esselle, M. Okoniewski, and M. A. Stuchly, "Analysis of sharp metal edges at 45° to the FDTD grid," *IEEE. Microwave Guided Wave Lett.*, vol. 9, pp. 221–223, June 1999.

[2] L. Cascio, G. Tardioli, T. Rozzi, and W. J. R. Hoefer, "A quasistatic modification of TLM at knife edge and 90° wedge singularities," *IEEE Trans. Microwave Theory Tech*, vol. 44, pp. 2519–2524, Dec. 1996.

[3] G. Mur, "The modeling of singularities in the finite-difference approximation of the time-domain electromagnetic field equations," *IEEE Trans. Microwave Theory Tech*, vol. 29, pp. 1073–1077, Oct. 1981.

[4] J. Fang and J. Ren, "A locally conformed finite-difference time-domain algorithm of modeling arbitrary shape planar metal strip," *IEEE Trans. Microwave Theory Tech.*, vol. 41, pp. 830–838, May 1993.

[5] I. J. Craddock and C. J. Railton, "Stable inclusion of a priori knowledge of field behavior in the FD-TD algorithm: Application to the analysis of microstrip lines," in *IEEE AP-S Int. Symp.*, Baltimore, MD, July 1996, pp. 1300–1303.

[6] J. Van Bladel, *Singular Electromagnetic Fields and Sources*. Oxford, U.K.: Clarendon, 1991, p. 121.

[7] X. Zhang, J. Fang, K. K. Mei, and Y. Liu, "Calculation of the dispersive characteristics of microstrips by the time-domain finite difference method," *IEEE Trans. Microwave Theory Tech.*, vol. 36, pp. 263–267, Feb. 1988.

[8] A. Taflove, *Computational Electromagnetics, The Finite-Difference Time-Domain Method*. Boston, MA: Artech House, 1995.